



HAL
open science

Estimation of the Absolute Orientation of a Five-link Walking Robot with Passive Feet

Yannick Aoustin, Gaëtan Garcia, Philippe Lemoine

► **To cite this version:**

Yannick Aoustin, Gaëtan Garcia, Philippe Lemoine. Estimation of the Absolute Orientation of a Five-link Walking Robot with Passive Feet. Armando Carlos de Pina Filho. Humanoid Robots: New Developments, I-Tech Education and Publishing, Vienna, Austria, Chap. 3, pp. 31-44, 2007, 978-3-902613-00-4. 10.5772/4859 . hal-00362625v1

HAL Id: hal-00362625

<https://hal.science/hal-00362625v1>

Submitted on 19 Feb 2009 (v1), last revised 18 Jan 2022 (v2)

HAL is a multi-disciplinary open access archive for the deposit and dissemination of scientific research documents, whether they are published or not. The documents may come from teaching and research institutions in France or abroad, or from public or private research centers.

L'archive ouverte pluridisciplinaire **HAL**, est destinée au dépôt et à la diffusion de documents scientifiques de niveau recherche, publiés ou non, émanant des établissements d'enseignement et de recherche français ou étrangers, des laboratoires publics ou privés.

Estimation of the Absolute Orientation of a Five-link Walking Robot with Passive Feet.

Yannick Aoustin, Gaëtan Garcia, Philippe Lemoine
*Institut de Recherche en Communications et Cybernétique de Nantes (IRCCyN),
École Centrale de Nantes, Université de Nantes, U.M.R. 6597, 1 rue de la Noë,
BP 92101, 44321 Nantes Cedex 3, France.
e-mail: surname.name@irccyn.ec-nantes.fr*

1. Introduction

One of the main objectives of current research on walking robots is to make their gaits more fluid by introducing imbalance phases. For example, for walking robots without actuated ankles, which are under actuated in single support, dynamically stable walking gaits have been designed with success (Aoustin & Formal'sky 2003; Chevallereau et al. 2003; Zonfrilli et al. 2002; Aoustin et al. 2006; Pratt et al. 2001; Westervelt et al.). Both the design of reference motions and trajectories and the control of the mechanism along these trajectories usually require the knowledge of the whole state of the robot. This state contains internal variables which are easy to measure using encoders for example, and also the absolute orientation of the robot with respect to the horizontal plane. For robots with unilateral constraints with the ground, it may not be possible to derive the latter information from internal measurements, as in the case of the absolute orientation of a biped in single support. Of course, technological solutions exist such as accelerometers, gyrometers, inertial units... But the implementation of these solutions is expensive and difficult.

In order to overcome these difficulties, we propose to use a state observer which, based on the measurements of the joint variables and on a dynamic model of the robot, provides estimates of the absolute orientation of the walking robot during imbalance phases. This strategy was first validated in simulation for a three link biped without feet, using nonlinear high gain observers and a nonlinear observer based on sliding modes with a finite time convergence (Lebastard et al. 2006a) and (Lebastard et al. 2006b), for walking gaits composed of single support phases and impacts. The main drawback with this family of observers is that, when only some of the degrees of freedom are measured, a state coordinates transformation is necessary to design their canonical form (Gauthier & Bornard 1981; Krener & Respondek 1985; Bornard & Hammouri 1991; Plestan & Glumineau 1997).

In this chapter, the observer is an extended Kalman filter and it is applied to *SemiQuad*, a prototype walking robot built at our institute. *SemiQuad* is a five link mechanism with a platform and two double-link legs. It is designed to study quadruped gaits where both front legs (resp. rear legs) have identical movements. Its unique front leg (resp. rear leg) acts as the two front legs (resp. rear legs) of the quadruped, so that *SemiQuad* can be considered as an implementation of a virtual

quadruped, hence its name. The legs have passive (uncontrolled) feet that extend in the frontal plane. Due to this, the robot is stable in the frontal plane. Four motors located in haunches and knees drive the mechanism. The locomotion of the prototype is a planar curvet gait. In double support, our prototype is statically stable and over actuated. In single support, it is unstable and under actuated.

The reference walking gaits have been designed using an intuitive strategy which is such that the absolute orientation is not required. Still, it contains imbalance phases during which the observer can be used, and its results evaluated. The estimation results being correct, such an observer can be used for contexts where the absolute angle is necessary. Furthermore, the idea can be useful for other types of walking robots, such as bipeds with imbalance phases.

The organization of this chapter is the following. Section 2 is devoted to the model of *SemiQuad*. It also contains the data of its physical parameters. The intuitive gaits which were designed for *SemiQuad* are presented in section 3. The statement of the problem of estimation of the absolute orientation of *SemiQuad* is defined in Section 4. Simulation results and experimental results are presented in section 5. Section 6 presents our conclusions and perspectives.

2. Presentation and dynamic models of *SemiQuad*

2.1 *SemiQuad*

The prototype (see figure 1) is composed of a platform and two identical double-link legs with knees. The legs have passive (uncontrolled) feet that extend in the frontal plane. Thus, the robot can only execute 2D motions in the sagittal plane, as considered here. There are four electrical DC motors with gearbox reducers to actuate the haunch joints between the platform and the thighs and the knee joints. Using a dynamic simulation, we have chosen parameters of the prototype (the sizes, masses, inertia moments of the links) and convenient actuators. The parameters of the four actuators with their gearbox reducers are specified in Table 1. The lengths, masses and inertia moments of each link of *SemiQuad* are specified in Table 2.

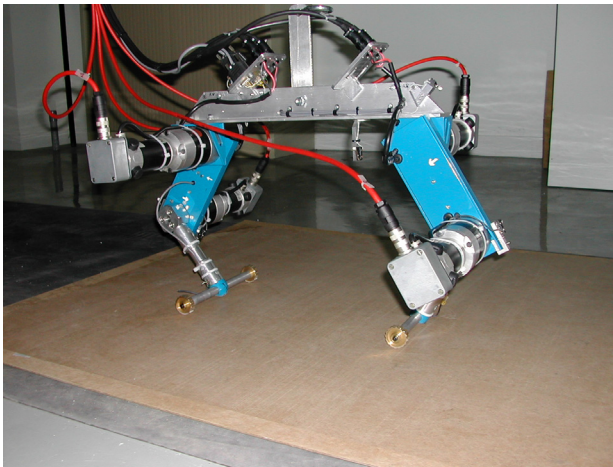


Fig. 1. Photography of *SemiQuad*.

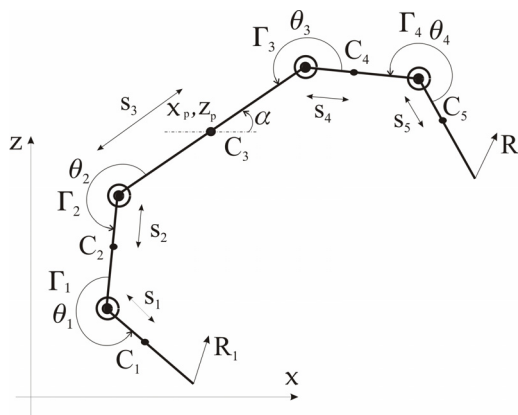
DC motor +gearbox	length (m)	mass (kg)	gearbox ratio	Rotor inertia (kg.m ²)	Electromagnetical torque constant (N.m)/A
in haunch	0.23	2.82	50	3.25 10 ⁻⁵	0.114
In knee	0.23	2.82	50	2.26 10 ⁻⁵	0.086

Table 1. Parameters of actuators

physical parameters of each link	mass (kg)	length (m)	Center of mass locations (m)	Moment of inertia (kg.m ²) around the center of mass C_i ($I=1,\dots,5$)
links 1 and 5: shin link 3: platform +actuators in each haunch	$m_1 = m_5 = 0.40$ $m_3 = 6.618$	$l_1 = l_5 = 0.15$ $l_3 = 0.375$	$s_1 = s_5 = 0.083$ $s_3 = 0.1875$	$I_1 = I_5 = 0.0034$ $I_3 = 0.3157$
links 2 and 4: thigh +actuators in each knee	$m_2 = m_4 = 3.21$	$l_2 = l_4 = 0.15$	$s_2 = s_4 = 0.139$	$I_2 = I_4 = 0.0043$

 Table 2. Parameters of *SemiQuad*

The maximum value of the torque in the output shaft of each motor gearbox is 40 N.m . This saturation on the torques is taken into account to design the control law in simulation and in experiments. The total mass of the quadruped is approximately 14 kg. The four actuated joints of the robot are each equipped with one encoder to measure the angular position. The angular velocities are calculated using the angular positions. Currently the absolute platform orientation angle α (see figure 2) is not measured. As explained before, the proposed walking gait does not require this measurement. Each encoder has 2000 pts/rev and is attached directly to the motor shaft. The bandwidth of each joint of the robot is determined by the transfer function of the mechanical power train (motors, gearboxes) and the motor amplifiers that drive each motor. In the case of *SemiQuad*, we have approximately a 16 Hz bandwidth in the mechanical part of the joints and approximately 1.7 kHz for the amplifiers. The control computations are performed with a sample period of 5 ms (200 Hz). The software is developed in C language.


 Fig. 2. *SemiQuad*'s diagram: generalized coordinates, torques, forces applied to the leg tips, locations of mass centers.

2.2 Dynamic model of *SemiQuad*

Figure 2 gives the notations of the torques, the ground reactions, the joint variables and the Cartesian position of the platform. Using the equations of Lagrange, the dynamic model of *SemiQuad* can be written:

$$D_e \ddot{q}_e + H_e \dot{q}_e + G_e = B_e \Gamma + D_{R_1} R_1 + D_{R_2} R_2 \quad (1)$$

with, $q_e := [q^T \ x_p \ z_p]^T$. The vector q is composed of the joint actuated variables and the absolute orientation of the platform, $q := [\theta_1 \ \theta_2 \ \theta_3 \ \theta_4 \ \alpha]^T$; (x_p, z_p) are the Cartesian coordinates of the platform center. The joint angle variables are positive for counter clockwise motion. $D_e(q)$ (7×7) is the inertia positive definite matrix. The matrix $H_e(q, \dot{q})$ (7×7) represents the Coriolis and centrifugal forces and $G_e(q)$ (7×1) is the vector of the gravity forces. B_e is a constant matrix composed of ones and zeros. Each matrix $D_{R_j}(q)$ (7×2) ($j = 1, 2$) is a jacobian matrix which represents the relation between feet Cartesian velocities and angular velocities. It allows to take into account the ground reaction R_j on each foot. If foot j is not in contact with the ground, then $R_j = [0, 0]^T$. The term $\Gamma := [\Gamma_1 \ \Gamma_2 \ \Gamma_3 \ \Gamma_4]^T$ is the vector of four actuator torques. Let us assume that during the single support, the stance leg acts as a pivot joint. Our hypothesis is that the contact of the swing leg with the ground results in no rebound and no slipping of the swing leg. Then, in single support, equation (1) can be simplified and rewritten as:

$$D\ddot{q} + H\dot{q} + G = B\Gamma \quad (2)$$

As the kinetic energy $K = \frac{1}{2} \dot{q}^T D \dot{q}$ does not depend on the choice of the absolute frame (see (Spong, M. & Vidyasagar M. 1991)) and furthermore variable α defines the absolute orientation of *SemiQuad*, the inertia matrix D (5×5) does not depend on α , and then $D = D(\theta_1, \theta_2, \theta_3, \theta_4)$. As for the case of equation (1), the matrix $H(q, \dot{q})$ (5×5) represents the Coriolis and centrifugal forces and $G(q)$ (5×1) is the vector of gravity forces. B is a constant matrix composed of ones and zeros. Equation (2) can be written under the following state form:

$$\dot{x} = \begin{bmatrix} \dot{q} \\ D^{-1} (-D\dot{q} - G + B\Gamma) \end{bmatrix} = f(x) + g(q_{rel})\Gamma \quad (3)$$

With $x = [q^T \ \dot{q}^T]^T$ and the joint angle vector $q_{rel} = [\theta_1 \ \theta_2 \ \theta_3 \ \theta_4]^T$. The state space is defined as $x \in X \subset \mathbb{R}^{10} = \left\{ x = [q^T \ \dot{q}^T]^T \mid |\dot{q}| < \dot{q}_M < \infty; q \in]-\pi, \pi]^5 \right\}$. From these definitions, it is clear that all state coordinates are bounded.

2.3 Discrete Model

Our objective is to design an extended Kalman filter with a sampling period Δ to observe the absolute orientation α . Then it is necessary to find a discrete model equivalent to (3). A

possible solution is to write $\dot{x} \approx \frac{x_{k+1} - x_k}{\Delta}$ and (3) becomes:

$$x_{k+1} = x_k + \Delta(f(x_k) + g(q_{relk})\Gamma_k) \quad (4)$$

For *SemiQuad*, we have preferred to sample the generalized coordinates and their velocities using approximations to a different order by a Taylor development:

$$x(t + \Delta) = x(t) + \Delta\dot{x}(t) + \Delta^2 \frac{\ddot{x}(t)}{2!} + \dots + \Delta^n \frac{x^{(n)}(t)}{n!} + \varepsilon, \quad (5)$$

From (5), developments to second order and first order have been used for the generalized coordinates and their velocities, respectively. Limiting the order where possible limits the noise, but using second order developments for position variables introduces their second order derivative and allows to make use of the dynamic model.

$$\begin{pmatrix} q_{k+1} \\ \dot{q}_{k+1} \end{pmatrix} \approx \begin{pmatrix} q_k \\ \dot{q}_k \end{pmatrix} + \Delta \begin{pmatrix} \dot{q}_k \\ \ddot{q}_k \end{pmatrix} + \frac{\Delta^2}{2} \begin{pmatrix} \ddot{q}_k \\ 0_{5 \times 1} \end{pmatrix} \quad (6)$$

With this method, a discrete model of (3) is calculated. If we add the equation corresponding to the measurement of the joint angles, we obtain the following system:

$$\begin{aligned} x_{k+1} &= f_s(x_k, \Gamma_k) \\ y_k &= h(x_k) = (\theta_1 \quad \theta_2 \quad \theta_3 \quad \theta_4)^T = Cx_k \quad \text{with } C = I_{4 \times 4} \end{aligned} \quad (7)$$

2.4 Impulsive impact equation

The impact occurs at the end of the imbalance phase, when the swing leg tip touches the ground, *i.e.* :

$x \in S = \{x \in X \mid q = q_f\}$ where q_f is the final configuration of *SemiQuad*. The instant of impact is denoted by T_i . Let us use the index 2 for the swing leg, and 1 for the stance leg during the imbalance phase in single support. We assume that:

- ◆ the impact is passive, absolutely inelastic;
- ◆ the swing leg does not slip when it touches the ground;
- ◆ the previous stance leg does not take off;
- ◆ the configuration of the robot does not change at the instant of impact.

Given these conditions, at the instant of an impact, the contact can be considered as impulsive forces and defined by Dirac delta-functions $R_j = I_{R_j} \Delta(t - T_i)$ ($j=1, 2$). Here

$I_{R_j} = [I_{R_{j1}} \quad I_{R_{j2}}]^T$, is the vector of the magnitudes of the impulsive reaction in leg j (Formal'sky 1974). The impact model is calculated by integrating (1) between T_i^- (just before impact) and T_i^+ (just after impact). The torques provided by the actuators at the joints, and Coriolis and gravity forces, have finite values, thus they do not influence the impact. Consequently the impact equation can be written in the following matrix form:

$$D_e(q)(\dot{q}_e^+ - \dot{q}_e^-) = D_{R_1}(q)I_{R_1} + D_{R_2}(q)I_{R_2} \quad (8)$$

Here, q is the configuration of *SemiQuad* at $t = T_i$, \dot{q}_e^- and \dot{q}_e^+ are the angular velocities just before and just after impact, respectively. Furthermore, the velocity of the stance leg tip before impact is null. Then we have:

$$D_{R_1}^T \dot{q}_e^+ = 0_{2 \times 1} \quad (9)$$

After impact, both legs are stance legs, and the velocity of their tip becomes null:

$$\begin{pmatrix} D_{R_1}^T \\ D_{R_2}^T \end{pmatrix} \dot{q}_e^+ = 0_{4 \times 1} \quad (10)$$

3. Walking gait strategy for *SemiQuad*

By analogy with animal gaits with no flight phase, *SemiQuad* must jump with front or back leg to realize a walking gait. There is no other way to avoid leg sliding. Then it is necessary to take into account that *SemiQuad* is under actuated in single support and over actuated in double support. Let us briefly present the adopted strategy to realize a walking gait for *SemiQuad*. It was tested first in simulation to study its feasibility and then experimentally (Aoustin et al. 2006). A video can be found on the web page <http://www.irccyn.ec-nantes.fr/irccyn/d/en/equipres/Robotique/Themes/Mobile>. Figure 4 represents a sequence of stick configurations for one step to illustrate the gait. Let us consider half step n as the current half step, which is composed of a double support, a single support on the rear leg and an impact on the ground. During the double support, *SemiQuad* has only three degrees of freedom. Then its movement can be completely prescribed with the four actuators. A reference movement is chosen to transfer the platform centre backwards. This is done by defining a polynomial of third order for both Cartesian coordinates x_p and z_p . The coefficients of these polynomials are calculated from a choice of initial and final positions, of the initial velocity and an intermediate position of the platform centre. The reference trajectories for the four actuated joint variables are calculated with an inverse geometric model. Then, by folding and immediately thrusting the front leg, the single support phase on the rear leg starts. During this imbalance phase, *SemiQuad* has five degrees of freedom and its rotation is free around its stance leg tip in the sagittal plane. Reference trajectories are specified with third order polynomial functions in time for the four actuated inter-link angles. However, the final time T_p of these polynomial functions is chosen smaller than the calculated duration T_{ss} of the single support phase, such that before impact the four desired inter-link angles (θ_{id} $i = 1, \dots, 4$) become constant. Using this strategy, we obtain the desired final configuration of our prototype before the impact even if T_{ss} is not equal to the expected value.

$$\begin{aligned} \theta_{id} &= a_0 + a_1 t + a_2 t^2 + a_3 t^3 & \text{if } t < T_p \\ \theta_{id} &= \theta_{ie}(T_p) & \text{if } T_p \leq t \leq T_{ss} \end{aligned} \quad (11)$$

The coefficients of these polynomials are calculated from a choice of initial, intermediate and final configurations and of the initial velocity for each joint link. Just after impact, the next half step begins and a similar strategy is applied (figure 4). The tracking of the reference trajectories is achieved using a PD controller. The gains, which were adjusted using pole placement, were tested in simulation and in experiments. Figure 3 shows the evolutions of the absolute orientation variable $\alpha(t)$ and its velocity $\dot{\alpha}(t)$, obtained from the simulation of *SemiQuad* for five steps. These graphs clearly show that the dynamics of the absolute orientation cannot be neglected in the design of a control law based on a state feedback. The durations of the double support phase and the single support phase are 1.5 s and 0.4 s respectively.

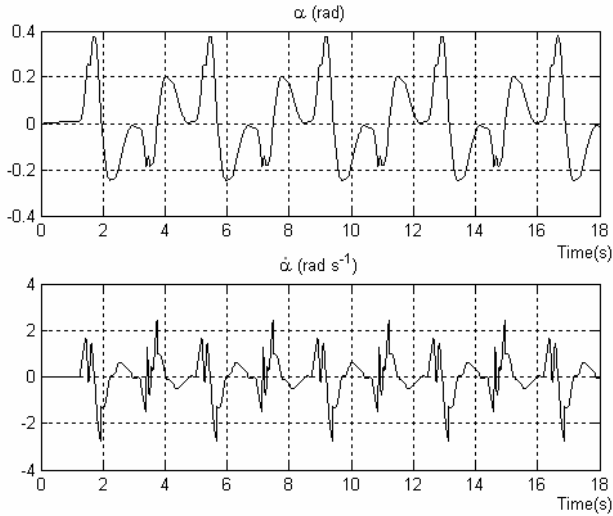


Fig. 3. Evolution of $\alpha(t)$ and $\dot{\alpha}(t)$ in simulation during the walking gait for five steps.

4. Observation of the absolute orientation of *SemiQuad*

System (3) is generically observable if the following matrix O has a full rank (see (Plestan & Glumineau 1997)), which is equal to 10, with (k_1, \dots, k_p) the p observability indexes.

$$O = \begin{pmatrix} dh_1 & \dots & dL_f^{k_1-1}h_1 & \dots & dh_p & \dots & dL_f^{k_p-1}h_p \end{pmatrix} \quad (12)$$

where dh is the gradient vector of function h (see system (7)) with respect to the state vector x , and $dL_f h$ is the Lie derivative of h along the vector field f . We have also checked that the equivalent property is satisfied by the discrete model. This means that, at each sampling time t_k , it is possible to find an observability matrix with 10 independent rows or columns.

Having checked system observability, we propose an Extended Kalman Filter to observe the absolute orientation. The design of this Extended Kalman Filter is now described.

In practice, due to uncertainty in the determination of parameters and to angular measurement errors, system (3), and of course system (7), are only approximations. A standard solution is to represent modelling and measurement errors as additive noises disturbing the system.

Let us consider the associated "noisy" system:

$$\begin{aligned} x_{k+1} &= f_s(x_k, \Gamma_k) + \alpha_k \\ y_k &= C(x_k) = (\theta_1 \quad \theta_2 \quad \theta_3 \quad \theta_4)^T + \beta_k \end{aligned} \quad (13)$$

In the case of a linear system, if α_k and β_k are white Gaussian noises, mutually independent and independent of x , the Kalman filter is an optimal estimator. When the system is not linear, it is possible to use the Extended Kalman Filter (EKF) by linearizing the evolution equation f_s and the observation equation (which is in our case linear) around the current state estimate. Although convergence and optimality are no longer guaranteed, the

interest and the effectiveness of the Extended Kalman Filter have been proved in many experimental cases. The EKF is very often used as a state observer (Bonnifait & Garcia 1998).

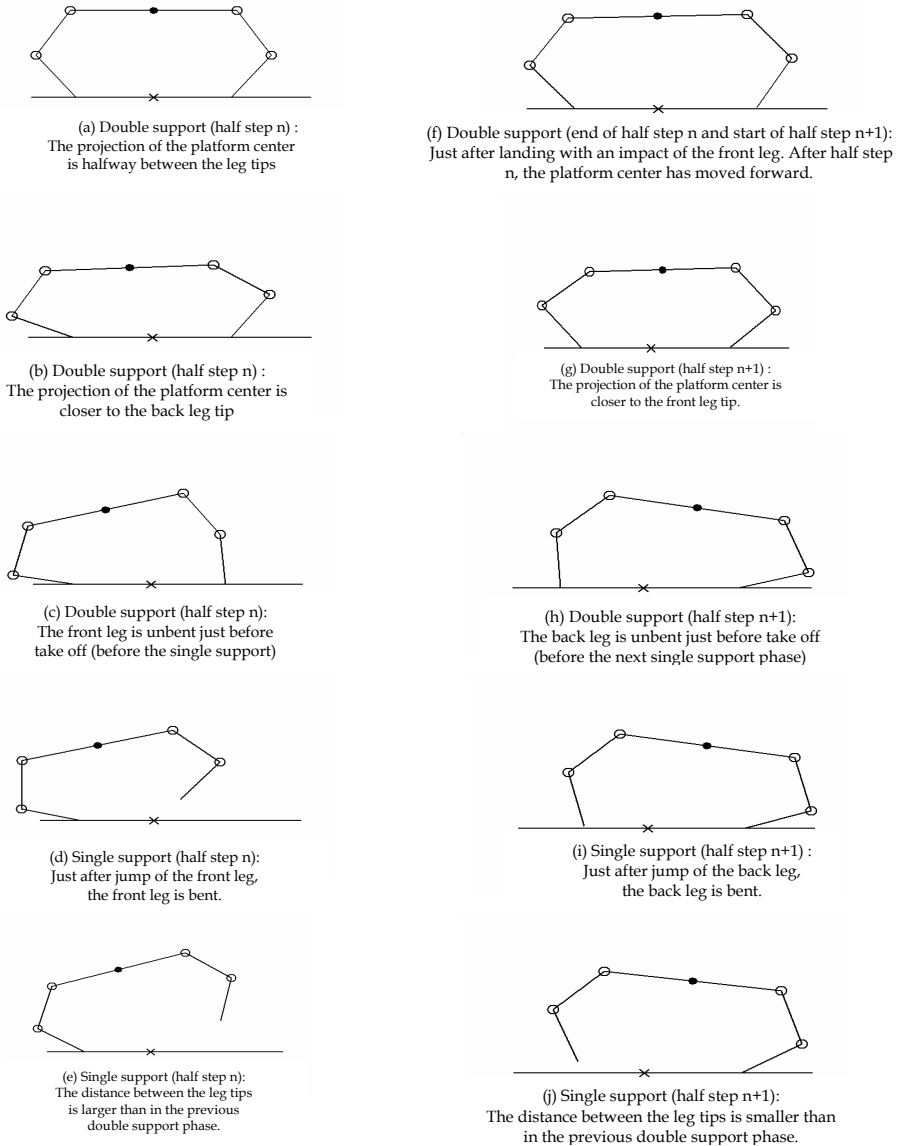


Fig. 4. Plot of half steps n and $n+1$ of *SemiQuad*. as a sequence of stick figures.

In the case of our system, the equations of the EKF are:

- *a priori* estimation: uses data available before t_{k+1}

$$\begin{aligned}\hat{x}_{k+1}^- &= f_s(\hat{x}_k, \Gamma_k) \\ P_{k+1}^- &= A_k P_k A_k^T + Q_\alpha\end{aligned}\quad (14)$$

- *a posteriori* estimation: uses data available at t_{k+1}

$$\begin{aligned}\hat{x}_{k+1} &= \hat{x}_{k+1}^- + K_{k+1} (y_{k+1} - Cx_{k+1}^-) \\ P_{k+1} &= (I_{10 \times 10} - K_{k+1} C) P_{k+1}^-\end{aligned}\quad (15)$$

with:

$$A_k = \left(\frac{\partial f_s}{\partial x} \right)_{x=\hat{x}_k} \quad \text{and} \quad K_{k+1} = P_{k+1}^- C^T (C P_{k+1}^- C^T + Q_\beta)^{-1}$$

Here y_{k+1} are the measured joint variables, which are the first four components of vector x_k at time t_k , and \hat{x}_{k+1}^- is the *a priori* estimation of these joint variables. Q_α and Q_β are the covariance matrices of α_k and β_k , K is the Kalman gain and P the estimated covariance matrix of prediction (P^- at t_k) and estimation (P at t_k) errors.

5. Simulation and experimental results.

For the simulation and experimental tests, the physical parameters defined in section 2 are used. The sampling period Δ is equal to 5 ms. The incremental encoders having $N=2000$ points per revolution, the variance of measurement is taken equal to $\pi^2 / (3\Delta N^2) = 8.225 \cdot 10^{-4}$. The errors of incremental encoders being independent, we have chosen $Q_\beta = 8.225 \cdot 10^{-4} I_{4 \times 4}$. The components of Q_α for the configuration variables are determined by trial and error from simulation and experimental results. The components of Q_α for velocity variables are derived from the values for position variables, taking into account the sampling period, and are larger than those corresponding to position variables.

$$Q_\alpha = \begin{pmatrix} 3.0 \cdot 10^{-10} I_{5 \times 5} & 0_{5 \times 5} \\ 0_{5 \times 5} & 3.0 \cdot 10^{-5} I_{5 \times 5} \end{pmatrix}$$

The initialization of the covariance matrix P takes into account a determination of α less precise and fixes the variances on the velocities, as for Q_α , taking into account of the sampling period.

$$P_0 = \begin{pmatrix} 8 \cdot 10^{-10} I_{4 \times 4} & 0_{4 \times 1} & 0_{4 \times 5} \\ 0_{1 \times 4} & 1.7 \cdot 10^{-5} & 0_{1 \times 5} \\ 0_{5 \times 4} & 0_{5 \times 1} & 5 \cdot 10^{-2} I_{5 \times 5} \end{pmatrix}$$

All the tests in simulations and in experiments were done following the scheme of figure 5. In simulations, the joint variables θ_i and their velocities $\dot{\theta}_i$ ($i=1,2,3,4$) obtained by integration of the direct dynamic model of *SemiQuad* and the control torques Γ_i ($i=1,2,3,4$) are the inputs of the Extended Kalman Filter. For the experimental tests, the joint variables θ_i ($i=1,2,3,4$) are measured and differentiated to obtain the velocities $\dot{\theta}_i$. These eight variables, together with the four experimental torques Γ_i ($i=1,2,3,4$) are the inputs of the Extended Kalman Filter. In both cases, the state vector $[\theta_1 \ \theta_2 \ \theta_3 \ \theta_4 \ \alpha \ \dot{\theta}_1 \ \dot{\theta}_2 \ \dot{\theta}_3 \ \dot{\theta}_4 \ \dot{\alpha}]^T$ is estimated.

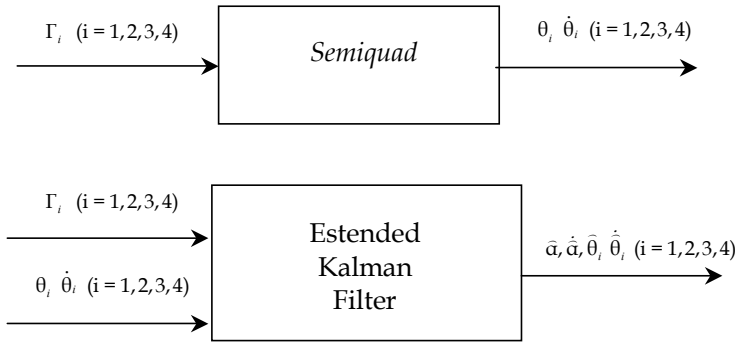


Fig. 5. Principle of tests of the Extended Kalman Filter with *SemiQuad*.

5.1 Simulation results

Figure 6 shows the evolution of the estimated and real orientations of the platform during a single support phase of the cyclic walking gait of *SemiQuad*. The initial error, which has been set to 0.0262 rad (1.5 degree), is rapidly reduced, and the estimated orientation converges towards the real orientation. Let us notice that a maximum value of 1.5 degree for the initial error is reasonable because experimentally $\hat{\alpha}(0)$ is determined by the geometric model at the end of the previous double support.

In the model used by the observer, we do not consider any friction. We have performed robustness tests of our estimator by adding a viscous friction, $\Gamma_i = F_v \dot{\theta}_i$ ($i=1,2,3,4$), and a Coulomb friction $\Gamma_i = F_s \dot{\theta}_i$ ($i=1,2,3,4$) to the simulation model. Figure 7 shows the estimated and real orientations of the platform of *SemiQuad* in the case when a viscous friction is added. The coefficient F_v equals to 0.1 N.m.s/rad. Similarly, figure 8 shows the estimated and the real orientations of the platform of *SemiQuad* in the case of a Coulomb friction, with a coefficient F_s equal to 0.2 N.m. Last robustness test (figure 9) presents the estimated and real orientations of the platform of *SemiQuad* with an inertia reduced by 5% for the platform in the simulator. In practice, 5% precision on inertia is feasible (see identification results in (Lydoire & Poignet 2003)).

From these robustness tests, we can conclude that we have no finite time convergence. However, the final relative errors of the estimated orientations of the platform of *SemiQuad* are small. Since it will be possible to update the initial condition of the estimator during the next double support phase, with the measurements of the encoders and the geometrical relations, such errors are not a problem.

5.2 Experimental results

At each step, the estimator is initialized with the configurations and the velocities at the end of the previous double support phase. At each sampling time, velocities are obtained by the usual differentiation operation $\dot{\theta}_i = \frac{\theta_i(k\Delta) - \theta_i((k-1)\Delta)}{\Delta}$ ($i=1,2,3,4$). No filtering is applied to smooth the measured joint variables θ_i , their velocities $\dot{\theta}_i$ and the four torques Γ_i ($i=1,2,3,4$).

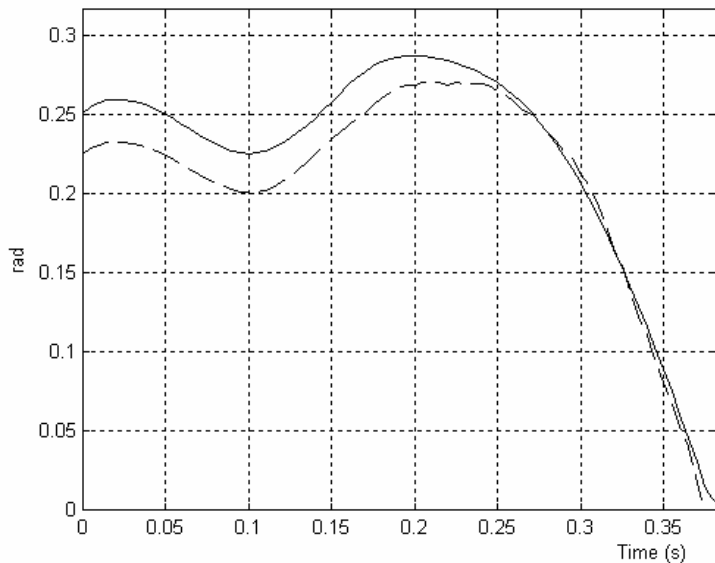


Fig. 6. Absolute orientation $\alpha(t)$ of the platform: real (solid) and estimated (dashed).

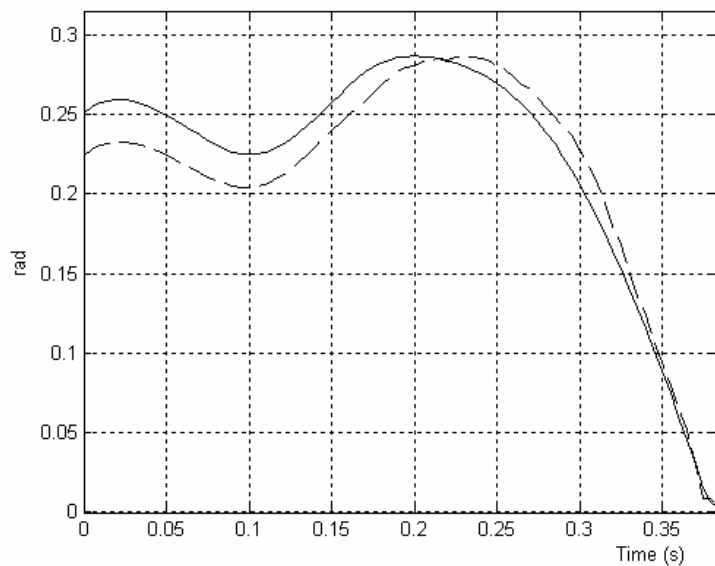


Fig. 7. Absolute orientation $\alpha(t)$ of the platform: real (solid) and estimated (dashed), with a supplement viscous friction.

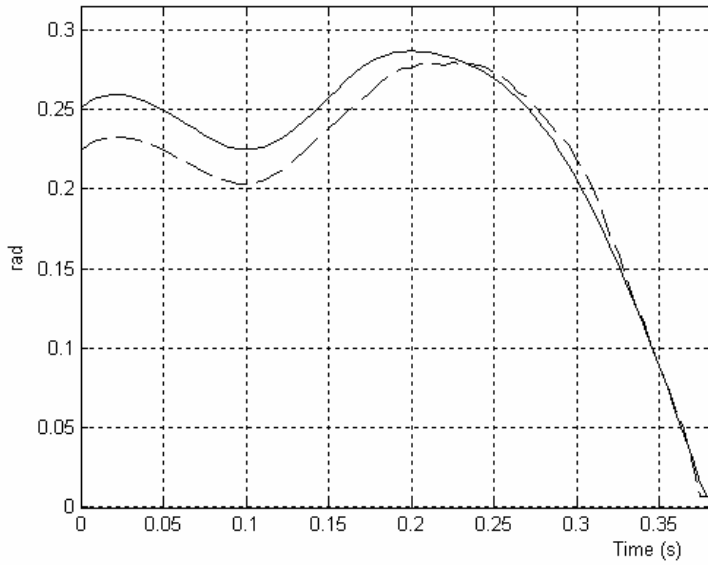


Fig. 8. Absolute orientation $\alpha(t)$ of the platform: real (solid) and estimated (dashed), with a supplement Coulomb friction.

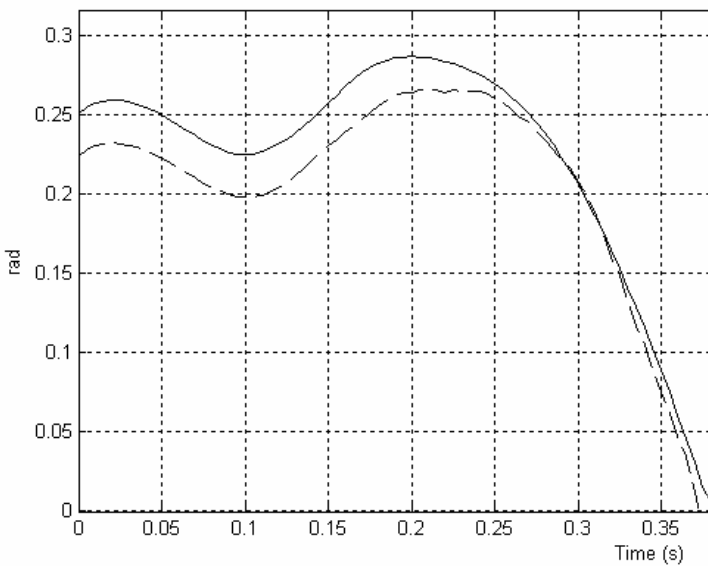


Fig. 9. Absolute orientation $\alpha(t)$ of the platform: real (solid) and estimated (dashed), with an error on the inertia of the platform.

Figure 10 shows the estimation of the absolute orientation of the platform $\alpha(t)$. The duration of the single support phase is 15% smaller than in simulation. It can probably be explained by the fact that our knowledge of the physical parameters of the robot is not perfect, and that we neglected effects such as friction in the joints.

Currently, there is no experimental measured data about the evolution of $\alpha(t)$ in single support, because *SemiQuad* is not equipped with a sensor such as a gyrometer or a gyroscope. However, in double support, using the geometric and kinematic models it is possible to calculate $\alpha(t)$ and $\dot{\alpha}(t)$. In addition to providing initial conditions for the observer, this also allows to calculate the orientation at the end of the single support phase, just after impact. The corresponding value is displayed as a star on the next graph, and is equal to 0.01 rad (0.57 degree). The difference between this value and the estimated value at the same instant is almost 3 degrees.

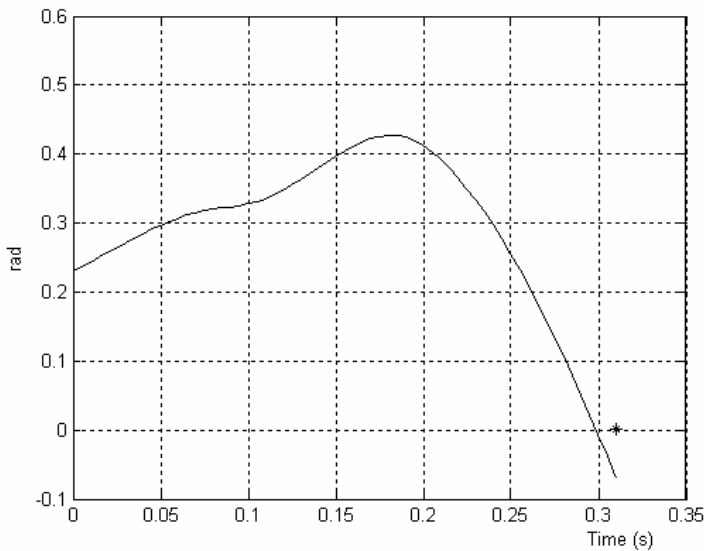


Fig. 10. Estimation of the absolute orientation $\alpha(t)$ of the platform using the experimental data.

6. Conclusion

An application of the digital Extended Kalman Filter has been presented for the problem of estimating the absolute orientation of *SemiQuad*, a 2D dynamically stable walking robot. There are some differences between simulations and experiments, but the results still prove the ability of our observer to yield a short term estimation of the orientation of the robot. The precision is sufficient for the estimation to be useful for calculating the dynamic model and monitoring the balance of the robot. This task is important for *SemiQuad*, and vital for bipeds, to which the idea is also applicable (see Lebastard, Aoustin, & Plestan 2006 for a different type of observer). Given the possibility to re-initialize the observer at each double support phase, even if very short, as it can be for bipeds, the observer can provide the absolute orientation over time without the use of any additional sensor, which was the goal of our work.

In a near future, we plan to equip *SemiQuad* with a gyrometer to fully evaluate the performance of our estimator over time. Our perspective is to use the estimated orientation in advanced feedback controllers.

7. References

- Aoustin, Y. & Formal'sky, A. (2003). Control design for a biped: Reference trajectory based on driven angles as function of the undriven angle, *Journal of Computer and System Sciences International*, Vol. 42, No. 4, (July-August 2003) 159-176.
- Chevallereau, C.; Abba, G.; Aoustin, Y.; Plestan, F.; Westervelt, E. R.; Canudas de Wit, C. & Grizzle, J. W. (2003). Rabbit: A testbed for advanced control theory, *IEEE Control Systems Magazine*, Vol. 23, (October 2003) No. 5, 57-78.
- Zonfrilli, F.; Oriolo, M. & Nardi, T. (2002). A biped locomotion strategy for the quadruped robot Sony ers-210, *Proceedings of IEEE Conference on Robotics and Automation*, pp. 2768-2774.
- Aoustin, Y.; Chevallereau, C. & Formal'sky, A. (2006). Numerical and experimental study of the virtual quadruped-SemiQuad, *Multibody System Dynamics*, Vol. 16, 1-20.
- Pratt, J.; Chew, C. M.; Torres, A.; Dilworth, P. & Pratt, G. (2001). Virtual model control: an intuitive approach for bipedal locomotion, *International Journal of Robotics Research*, Vol. 20, No. 2, 129-143.
- Westervelt, E. R.; Grizzle, J. W. & Koditschek, D. E. (2003). Hybrid zero dynamics of planar biped walkers, *IEEE Transactions on Automatic Control*, Vol. 48, No. 1, (February 2003) 42-56.
- Lebastard, V.; Aoustin, Y. & Plestan, F. (2006). Observer-based control of a walking biped robot without orientation measurement, *Robotica*, Vol. 24, 385-400.
- Lebastard, V.; Aoustin, Y. & Plestan F. (2006) . Absolute orientation estimation for observer-based control of a five-link biped robot, *Springer Verlag Series Notes on Control and Information Sciences*, Editor: K. Kozlowski, Springer, vol. 335, Lecture Notes in Control and Information Sciences, 2006.
- Gauthier, J.P. & Bornard, G. (1981). Observability for any $u(t)$ of a class of nonlinear system. *IEEE Transactions on Automatic Control*, 26(4): 922-926.
- Krener, A. & Respondek, W. (1985). Nonlinear observers with linearization error dynamics, *SIAM Journal Control Optimization*, Vol. 2, 197-216.
- Bornard, G. & Hammouri, H. (1991). A high gain observer for a class of uniformly observable systems, *Proceedings of the 30th IEEE Conference on Decision and Control*, pp. 1494-1496.
- Plestan, F. & Glumineau, A. (1997). Linearisation by generalized input-output injection, *Systems and Control Letters*, Vol. 31, 115-128.
- Spong, M. & Vidyasagar M. (1991). Robot dynamics and control, *John Wiley*, New-York.
- Formal'sky, A. M. (1982). Locomotion of Anthropomorphic Mechanisms, *Nauka, Moscow* [In Russian], 368 pages.
- Bonnifait, P. & Garcia, G. (1998). Design and experimental validation of an odometric and goniometric localization system for outdoor robot vehicles, *IEEE Transactions on Robotics and Automation*, Vol. 14, No. 541-548.
- Lydoire, F. & Poignet, Ph. (2003). Experimental dynamic parameters identification of a seven dof walking robot, *Proceedings of the CLAWAR'03 Conferencel*, pp. 477-484.